The PET Radioligand [*carbonyl*-^{11}C]Desmethyl-WAY-100635 Binds to 5-HT$_{1A}$ Receptors and Provides a Higher Radioactive Signal Than [*carbonyl*-^{11}C]WAY-100635 in the Human Brain

Bengt Andrée, MD, PhD[1]; Christer Halldin, PhD[1]; Victor W. Pike, PhD[2]; Roger N. Gunn, PhD[2]; Hans Olsson, MD[1]; and Lars Farde, MD, PhD[1]

[1]*Psychiatry Section, Department of Clinical Neuroscience, Karolinska Hospital, Karolinska Institutet, Stockholm, Sweden; and* [2]*MRC Cyclotron Unit, Hammersmith Hospital, Imperial College School of Medicine, London, United Kingdom*

5-Hydroxytryptamine (serotonin)-1A (5-HT$_{1A}$) receptors are of key interest in research on the pathophysiology and treatment of psychiatric disorders. The PET radioligand [*carbonyl*-^{11}C]WAY-100635 (^{11}C-WAY), where WAY-100635 is ^{3}H-(*N*-(2-(1-(4-(2-methoxyphenyl)-1-piperazinyl)ethyl)-*N*-(2-pyridyl) cyclohexane-carboxamide, is commonly used for quantitation of 5-HT$_{1A}$ receptors in the human brain. The aim of this PET study was to compare ^{11}C-WAY with the putative metabolite and selective radioligand [*carbonyl*-^{11}C]desmethyl-WAY-100635 (^{11}C-DWAY). **Methods:** A PET examination was performed on each of 5 healthy male volunteers after intravenous injection of ^{11}C-WAY and ^{11}C-DWAY on separate occasions. Radioactive metabolites in plasma were determined with high-performance liquid chromatography. The plasma metabolite–corrected input function was used in a kinetic compartment analysis. The simplified reference tissue model and peak equilibrium method, using the cerebellum as reference region, was applied for comparison of data. **Results:** For both radioligands, the highest radioactivity was observed in the neocortex and the raphe nuclei, whereas radioactivity was low in the cerebellum. The regional binding potentials were similar for the 2 radioligands. The brain uptake was more than 2-fold higher for ^{11}C-DWAY than for ^{11}C-WAY, in part because of higher delivery (first-order rate constant K$_1$, 0.38 vs. 0.16). The time–activity curves were well described by a 3-compartment model for all regions, whereas uptake in the cerebellum could not be described by a 2-compartment model, supporting the existence of kinetically distinguishable nonspecific binding in the cerebellum or radioactive metabolites in the brain for both radioligands. Both radioligands were rapidly metabolized, and <10% of the radioactivity in plasma represented unchanged ^{11}C-WAY or ^{11}C-DWAY at 10 min after injection. The metabolic pattern was similar for both radioligands, with the formation of radiolabeled cyclohexanecarboxylic acid and more polar components. For ^{11}C-WAY, small amounts of an additional labeled metabolite comigrated with reference desmethyl-WAY-100635. **Conclusion:** The advantages of ^{11}C-DWAY over ^{11}C-WAY for research on central 5-HT$_{1A}$ receptors is supported by a significantly higher radioactivity signal at equipotent doses, providing improved imaging statistics and advantages in biomathematic modeling and the preclusion of ^{11}C-DWAY as a metabolite interfering with PET measurements.

Key Words: brain; human; PET; 5-hydroxytryptamine-1A receptors; WAY-100635; desmethyl-WAY-100635; kinetic modeling

J Nucl Med 2002; 43:292–303

A technique currently applied to examine the pathophysiology of neuropsychiatric disorders and to establish the pharmacology of central nervous system drugs is PET (*1*). The progress of PET for brain imaging is related to the development of suitable radioligands for the multitude of neuroreceptor subtypes that are expressed in the human brain.

Imaging of serotonin 5-hydroxytryptamine-1A receptors (5-HT$_{1A}$) is of high interest in research on the pathophysiology and treatment of anxiety, depression, and schizophrenia (*2–5*). Presynaptic 5-HT$_{1A}$ receptors mediate inhibition of 5-hydroxytryptamine release (*6*) and are highly concentrated on cell bodies in the raphe nuclei, whereas postsynaptic receptors are abundant in the neocortex, as shown by in vitro studies (*7*).

The 5-HT$_{1A}$ receptor has recently been characterized in the postmortem human brain using the receptor antagonist ^{3}H-(*N*-(2-(1-(4-(2-methoxyphenyl)-1-piperazinyl)ethyl)-*N*-(2-pyridyl) cyclohexane-carboxamide (WAY-100635), which binds selectively and with high affinity (dissociation constant [K$_d$], approximately 0.4 nmol/L) to this receptor subtype (*8,9*). Labeling of WAY-100635 in its carbonyl group with ^{11}C (half-life, 20.4 min) yields a radioligand

(Fig. 1) that accurately delineates the distribution of 5-HT$_{1A}$ receptors in the human brain (10).

[carbonyl-^{11}C]WAY-100635 (^{11}C-WAY) has been characterized and used for quantitative studies of 5-HT$_{1A}$ receptors in the brains of humans and other primates (11–15). A common quantitative approach has been to use the cerebellum as reference tissue for the free radioactivity concentration in brain because this region is almost devoid of 5-HT$_{1A}$ receptors. A consistent finding has been a significantly better description of the cerebellar time–radioactivity curves by a 3-compartment model (3-CM) than by a 2-compartment model (2-CM) (13–15). One hypothesis to explain the better fit of data using a 3-CM for the cerebellum is the existence of kinetically distinguishable nonspecific binding. An alternative explanation is that the observation may represent uptake of a radioactive metabolite (13,14). Interestingly, WAY-100635 labeling in the carbonyl position (10) gives radioactive metabolites, such as ^{11}C-cyclohexanecarboxylic acid and, to a low extent, [carbonyl-^{11}C]desmethyl-WAY-100635 (^{11}C-DWAY) (Fig. 1), that may contribute to radioactivity in the cerebellum (11,16,17).

The metabolite ^{11}C-DWAY has high affinity to 5-HT$_{1A}$ receptors (inhibitory concentration of 50% [IC$_{50}$], 1.4 nmol/L) and has recently been suggested as a putative radioligand for PET (11,18,19). One reason is that ^{11}C-DWAY has the possible advantage of not forming any further labeled metabolite that passes the blood–brain barrier other than ^{11}C-cyclohexanecarboxylic acid. The binding of ^{11}C-DWAY to central 5-HT$_{1A}$ receptors has been characterized by autoradiography and in preliminary PET studies in monkeys and humans (11,18,19).

The current PET study evaluated the prospects for using ^{11}C-DWAY as an alternative to ^{11}C-WAY for quantification of central 5-HT$_{1A}$ receptors in the human brain. Two- and 3-compartment analyses and 2 reference tissue approaches were applied in 5 healthy male volunteers to calculate rate constants and estimate regional radioligand binding in the brain. Radioactive metabolites in plasma were examined with high-performance liquid chromatography (HPLC).

MATERIALS AND METHODS

Subjects

The study was approved by the ethics and the radiation safety committees of the Karolinska Hospital. Six men (age range, 20–32 y) participated in 2 PET measurements after giving informed consent. One of the 6 men was excluded because of arterial blood-sampling failure. All men were healthy according to history, physical examination, psychiatric interview, blood and urine analysis, and MRI of the brain. All were nonsmokers and used no medication.

MRI and Head Fixation System

The MRI system was a 1.5-T Signa (General Electric Medical Systems, Milwaukee, WI). T2-weighted and proton density MR images of the brain were obtained for all participants. A head fixation system with an individual plaster helmet was used for the PET and MRI examinations to allow mastery of positioning between the 2 modalities and to ensure accuracy on repositioning (5,20). The helmet was made so that the plane defined by the external anatomic landmarks of the meatus acusticus externus and the lateral angle of the orbita was oriented along the expected image plane.

Radiochemistry

^{11}C-WAY (Fig. 1) was synthesized as described previously (9). The specific radioactivity of ^{11}C-WAY at the time of intravenous injection was between 47,138 and 75,332 GBq/mmol. The radioactivity injected ranged from 257 to 300 MBq, and the injected mass ranged from 1.7 to 2.6 μg.

^{11}C-DWAY (Fig. 1) was prepared by ^{11}C-acylation of the appropriate secondary amine precursor, as described previously (18). ^{11}C-DWAY was isolated by HPLC on a μBondapak C-18 column (Waters, Milford, MA) eluted with methanol and 0.1 mol/L ammonium formate. All chemicals were of analytic grade. The radiochemical purity, chemical purity, and specific radioactivity of each batch were determined by HPLC. The radiochemical purity of the final products was >99%. The specific radioactivity of ^{11}C-DWAY at the time of intravenous injection ranged from 25,942 to 41,736 GBq/mmol, and the radioactivity injected was between 157 and 306 MBq, corresponding to an injected mass of 3.1–4.6 μg.

Arterial Blood Sampling

To obtain the arterial input function, an automated blood sampling system was used during the first 5 min of each PET mea-
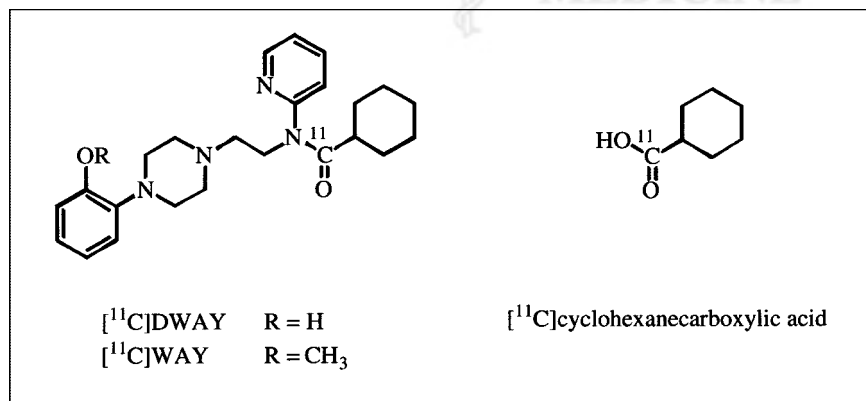

FIGURE 1. Chemical structure of [carbonyl-^{11}C]WAY-100635 (^{11}C-WAY) and 2 metabolites, [carbonyl-^{11}C]desmethyl-WAY-100635 (^{11}C-DWAY) and [carbonyl-^{11}C]cyclohexanecarboxylic acid.

surement (*21*). Subsequent arterial blood samples were taken manually at the midpoint of each frame until the end of the PET measurement (*22*). The experimentally defined difference between the appearance of radioactivity in the automated blood sampling system and brain was approximately 10 s.

Determination of Radioactive Metabolites in Plasma

The fractions of plasma radioactivity corresponding to unchanged ^{11}C-WAY and ^{11}C-DWAY were determined as described previously (*11*). In short, arterial blood samples (2 mL) were drawn at 4, 10, 20, 30, 40, 50, and 60 min after injection. The supernatant liquid obtained after centrifugation for 2 min was deproteinized with acetonitrile and analyzed by HPLC on a reverse-phase column (μBondapak C-18, 7.8 $\times$ 300 min, 10 μm) eluted at 6 mL/min over 9 min with acetonitrile and 0.01 mol/L phosphoric acid, using a gradient of 10:90 to 70:30 acetonitrile: phosphoric acid from 0 to 6.5 min and back to 10:90 at 7.5 min. The radioactivity in a certain fraction was expressed as the percentage of the total radioactivity in plasma (*14*).

PET Experimental Procedure

The PET system was an ECAT EXACT HR (CTI, Knoxville, TN/Siemens Medical Systems, Inc., Hoffman Estates, IL) that provided 47 sections with a center-to-center distance of 3.125 mm (*23*). The intrinsic spatial resolution was 3.6 mm in the imaging plane and 4.0 mm in full width at half maximum (FWHM) axially. With a Hanning filter, used for scatter correction, the reconstructed in-plain resolution was 5.5 mm in FWHM. Data were acquired in 3-dimensional mode. Scatter correction was performed as described in the literature, and attenuation correction was performed using the transmission scan data. The reconstructed volume was displayed as 47 transaxial sections with a section thickness of 3.125 mm.

Each subject was placed recumbent with his head in the PET system. To standardize the positioning of the cerebellum within a PET section and to avoid positioning this region at the edge of the axial field, anatomic landmarks were used together with the horizontal and vertical laser beams of the PET system.

Each subject was examined with PET on 2 occasions on the same day, once in the morning using ^{11}C-WAY and once in the afternoon using ^{11}C-DWAY. At least 4 h elapsed between the 2 measurements. The time between the 2 PET scans corresponded to more than 9 physical half-lives for ^{11}C (20.4 min). Residual radioactivity from the first PET measurement thus should not have interfered with the second PET measurement. In each PET measurement, the subject was placed recumbent with his head in the PET system. A cannula was inserted into the left brachial artery, and another cannula was inserted into the right antecubital vein. A sterile physiologic phosphate buffer (pH 7.4) solution containing ^{11}C-WAY or ^{11}C-DWAY was injected as a bolus during 2 s into the right antecubital vein. The cannula was then immediately flushed with saline (8 mL).

Brain radioactivity was measured in a series of 16 consecutive time frames for up to 69 min. The frame sequence consisted of three 1-min frames followed by four 3-min frames and nine 6-min frames.

Regions of Interest and Regional Radioactivity

Regions of interest (ROIs) were chosen for brain regions that are in the focus of research on schizophrenia, anxiety, and affective disorders. ROIs were defined for the neocortical regions, the cingulate cortex, the frontal and lateral temporal cortices, the insular cortex and the medial temporal cortices, the hippocampus, the raphe, and the cerebellar cortex. ROIs were delineated on MR images according to anatomic boundaries and were transferred to the corresponding PET images. However, the raphe nuclei were delineated directly on reconstructed PET images because this small structure cannot be distinguished on MR images.

The frontal and temporal cortices were drawn at the level of the basal ganglia, whereas the raphe nuclei were delineated at the level of the hippocampal formation. The ROIs for the cerebellar cortex and neocortical regions were drawn in 3 adjacent sections, and the raphe nuclei in 4 sections. Data were pooled so that the average radioactivity concentration for the whole volume of interest, and both hemispheres when applicable, was obtained.

The image matrix size was 128 $\times$ 128, and the pixel size was 2.0 mm. The pixel size was multiplied by the number of pixels of each ROI, plane, and subject to calculate the average ROI size. These values were 297 mm^2 for the cingulate cortex, 1,050 mm^2 for the frontal cortex, 1,260 mm^2 for the temporal cortex, 503 mm^2 for the insular cortex, 312 mm^2 for the hippocampus, 53 mm^2 for the raphe, and 690 mm^2 for the cerebellum.

Quantitative Analyses

To determine the rate constants describing the regional kinetics of ^{11}C-WAY and ^{11}C-DWAY, conventional 2-CMs and 3-CMs were fitted to the datasets. Parameters relating to binding and delivery of the tracers were derived from these rate constants. Statistical assessment of the residuals to the model fit allowed decisions to be made about the most appropriate compartment model configuration. In addition, 2 reference tissue approaches that do not require an arterial input function were applied to the datasets and regional binding potentials (BPs) were obtained.

Compartmental Analysis

Radioligand binding to 5-HT$_{1A}$ receptors was analyzed using the conventional compartmental model for PET ligand-receptor binding (Fig. 2). The 4 compartments correspond to the radioactivity concentrations of unchanged radioligand in plasma (C_p), free (unbound) radioligand in brain (Cf), nonspecifically bound radioligand in brain (C_{ns}), and radioligand specifically bound to receptors (C_b). All concentrations have the dimension nCi/mL.

A common assumption is that the concentrations of C_{ns} and Cf rapidly equilibrate to form an effective compartment (*24*) that corresponds to nondisplaceable radioligand in brain, or C_n. In this study, the resultant simplified model using 3 compartments and 4 first-order rate constants, K_1, k_2, k_3, and k_4 (*24–26*), was used to describe the time–radioactivity curves in brain regions known to contain 5-HT$_{1A}$ receptors. All compartments were assumed to be homogeneous in concentration. The model is described by the following set of differential equations:

$$dC_n(t)/dt = K_1 C_p(t) - (k_2 + k_3)C_n(t) + k_4 C_b(t) \quad \text{Eq. 1}$$

$$dC_b(t)/dt = k_3 C_n(t) - k_4 C_b(t) \quad \text{Eq. 2}$$

$$C_t(t) = C_n(t) + C_b(t), \quad \text{Eq. 3}$$

where $C_t(t)$ is the total radioactivity concentration in brain, corrected for the cerebral volume (CBV) as described further below.
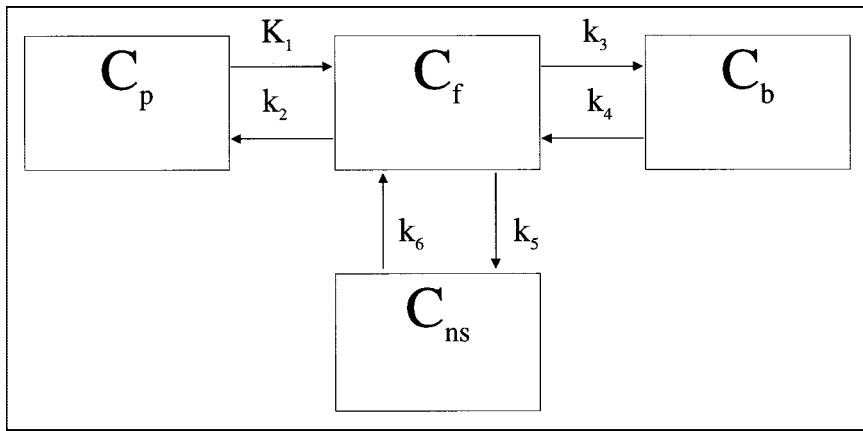
FIGURE 2. General compartmental configuration showing 2-CM and 3-CM.

The 4 rate constants were estimated by fitting the model in a least squares sense to the regional time–radioactivity curve (*27*). The differential equations were solved using a convolution approach (*28*). All data points were given equal weight. The time–radioactivity curves for unchanged ^{11}C-WAY and ^{11}C-DWAY in arterial plasma were used as input functions.

Reference Tissue Analysis

The cerebellum is a brain structure virtually devoid of 5-HT$_{1A}$ receptors (*9,29*). The radioactivity concentration in this reference region, $C_n(t)$, is estimated using the following 2 approaches.

Simplified Reference Tissue Model. The simplified reference tissue model, introduced by Lammertsma and Hume (*30*), is a 3-parameter model that provides increased convergence rates, including stability, compared with a previously developed 4-parameter model (*28*). By approximating the tissue ROI as a single tissue compartment, the model is reduced from 4 parameters to 3; the BP, the relative delivery to the ROI and compared with the reference tissue ($R_1 = K_1/K'_1$), and the efflux constant from brain to plasma (k_2). This model was used for the calculation of regional BP, which is referred to here as BP$_{SRTM}$.

Peak Equilibrium Method. The radioactivity in the cerebellum, $C_{cer}(t)$, was used to calculate $C_b(t)$, that is, $C_t(t) − C_{cer}(t)$, according to Equation 3, assuming that the radioligand time–radioactivity curves for free and nonspecific binding are identical in the reference and target tissues. The condition of peak equilibrium is defined as theoretically existing when the derivative for $C_b(t)$ is zero (*12*). This moment is called peak equilibrium because, theoretically, at that very moment the number of molecules associating to the receptors is equal to the number that dissociates from the receptors (*13*). At peak equilibrium, the ratio C_b/C_n is equal to the BP, which is referred to as BP$_{EQ}$.

BPs and Volumes of Distribution

The analyses used in this article are based on the injection of radioligand with high specific radioactivity. Under such conditions, the receptor density (B_{max}) and affinity (K_d) cannot be differentiated. The concept BP has been introduced as the ratio B_{max}/K_d, where B_{max} denotes the maximum concentration of binding sites and K_d denotes the apparent equilibrium dissociation rate constant (*13,25*). In the current comparison, the definition of the parameter BP also contains the tissue radioligand "free" fraction (f_2), and hence, BP = k_3/k_4 (= $f_2 B_{max}/K_d$).

A widely used quantitative approach has been to express radioligand binding in terms of distribution volume. Two such volumes are defined by Equations 4 and 5:

$$V_n = K_1/k_2 \qquad \text{Eq. 4}$$

and

$$V_t = (K_1/k_2) \times (1 + k_3/k_4). \qquad \text{Eq. 5}$$

V_n is the distribution volume in a brain region with only nondisplaceable binding and, thus, is devoid of specific binding sites. V_t is the total distribution volume. V_t was calculated by entering into Equations 4 and 5 the rate constants obtained from the 3-CM analysis.

In the current comparison of the 2 radioligands, regional BP was estimated in 3 ways: BP$_{3-CM}$, using the volume of distribution obtained from the 3-CM, and BP$_{SRTM}$ and BP$_{EQ}$, obtained from the 2 reference tissue approaches. The ratio of k_5 to k_6 for the cerebellum was used to calculate the "nonspecific" BP (BP$_{ns}$) for the cerebellum. $V_{cerebellum} = K_1/k_2$ is the distribution volume in a reference region with kinetically distinguishable nonspecific binding. For comparison of results, BP was also calculated from the compartment model fits as $V/V_{cerebellum} − 1$, where $V = K_1/k_2(1 + k_3/k_4)$ and $V_{cerebellum} = K_1/k_2(1 + k_3/k_4)$. The value thus derived should be most directly comparable with BP values calculated by the 2 reference methods.

Cerebellum as Reference Region

The cerebellum is a brain region with a low density of 5-HT$_{1A}$ receptors as supported by binding studies on postmortem human brain material (*7*), messenger RNA distribution (*31*), and receptor distribution in autoradiography studies (*9,29*).

In a region that is devoid of specific binding sites and thus does not have a specific binding compartment (C_b), a 2-CM with 2 rate constants should be sufficient to describe the time–activity curves (assuming rapid equilibration of the free and nonspecifically bound compartments). To evaluate the number of tissue compartments required to describe the cerebellum, we applied both a 2-compartment 2-parameter fit (K_1 and k_2) and a 3-compartment 4-parameter fit (K_1, k_2, k_5, and k_6) to the cerebellar cortex data (*12,22*). The 2 models were assessed statistically by application of the F test (*32*), the Akaike information criteria (*33*), and the Schwartz criteria (*34*) to the residual sum of squares of the model fits. The root mean square error was calculated using the equation $\sqrt{RSS/No. \text{Frames}}$, where RSS is the residual sum of squares.

Using a 2-CM in the cerebellum does not guarantee the ability to distinguish between free and nonspecific components as the 2 compartments. Nonspecific binding may have both a kinetically distinguishable component and, in addition, a rapidly equilibrating component as originally suggested (24).

Cerebral Blood Volume

Cerebral blood volume (CBV) correction was performed according to the following equation (22,28):

$$C_{ROI}(t) = (1 - V_b)C_t(t) + V_bC_a(t), \qquad \text{Eq. 6}$$

where $C_{ROI}(t)$ is the ROI concentration, V_b is the blood volume component, $C_t(t)$ is the tissue concentration, and $C_a(t)$ is the whole-blood concentration. A reference V_b of 4% was used in the kinetic analyses to correct for radioactivity in CBV (35). The calculated radioactivity contribution from CBV was subtracted from the regional time–radioactivity curves before the compartment analysis. The ROI and cerebellum curves were not corrected for blood volume before the simplified reference tissue model (SRTM) and peak equilibrium method were applied; a bias may thus be expected.

Radioligand Brain Delivery

The radioligand brain delivery of ^{11}C-WAY and ^{11}C-DWAY was compared and examined for the total brain. In addition, maximum uptake was calculated. This parameter includes clearance and binding, thus providing information on expected imaging statistics in a complete biologic system in vivo. The average radioactivity for 4 adjacent brain sections was calculated to determine total radioactivity in brain. The average concentration in the time frame corresponding to maximal radioactivity uptake was used and multiplied by the average total brain volume (set to 1,350 mL). The total radioactivity uptake was then compared with the injected radioactivity to calculate brain uptake in percentage of injected ^{11}C-WAY and ^{11}C-DWAY.

RESULTS

Each subject participated in 2 PET examinations on the same day, once with ^{11}C-WAY and once with ^{11}C-DWAY. For both radioligands, radioactivity appeared rapidly in the brain (Figs. 3A and 3B). The highest radioactivity concen-
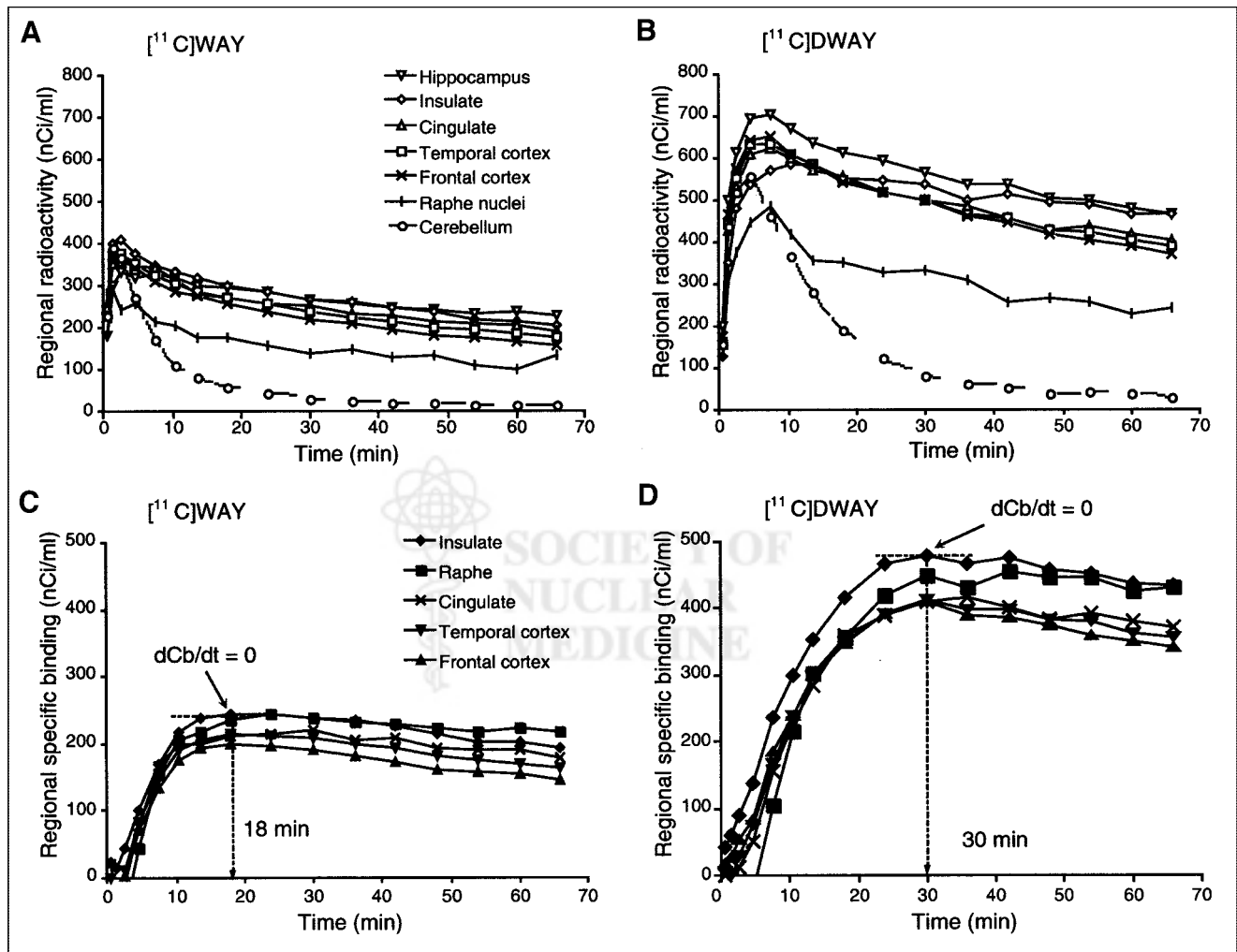

FIGURE 3. Time curves for regional brain radioactivity after intravenous injection of ^{11}C-WAY (A) and ^{11}C-DWAY (B), normalized to injected dose (300 MBq), and time curves for specific radioligand binding of ^{11}C-WAY (C) and ^{11}C-DWAY (D). dCb/dt indicates time of peak equilibrium.

tration was observed in the insular and medial temporal cortices (including the hippocampal formation), with a somewhat lower uptake in the raphe (Figs. 3A, 3B, and 4). A high signal was also notable in the cingulate, frontal, and lateral temporal cortices, whereas the signal in the cerebellum was low (Figs. 3 and 4).

The regional time–activity curves reached a peak at approximately 4 and 8 min after ^{11}C-WAY and ^{11}C-DWAY injection, respectively (Figs. 3A and 3B). The signal in all regions was about twice higher using ^{11}C-DWAY than using ^{11}C-WAY (Figs. 3A and 3B). The percentage of injected radioactivity in the brain at the time of maximal radioactivity uptake was 11.2 ± 1.9 for ^{11}C-DWAY and 4.6 ± 1.9 for ^{11}C-WAY (mean $\pm$ SD; $n = 5$).

Both radioligands were rapidly metabolized (Fig. 5A), and <10% of the radioactivity in plasma represented unchanged ^{11}C-WAY or ^{11}C-DWAY at 10 min after injection, as determined with HPLC (Fig. 5B). The HPLC chromatograms revealed similar polar labeled metabolites of ^{11}C-WAY and ^{11}C-DWAY and an identical comigration for the reference cyclohexanecarboxylic acid. For the ^{11}C-WAY radioligand only, there was an additional possible metabolite comigrating with DWAY (<2% of the parent radioligand at 10 min); however, the additional metabolite was not observed for all subjects.

Time–radioactivity curves for the neocortical regions and raphe could be described by the 3-CM. The average rate constants obtained from the 3-CM analysis are given in Table 1. A regression analysis of the rate constants obtained for ^{11}C-WAY and ^{11}C-DWAY was performed on all ROIs except the cerebellum (Fig. 6A), which was analyzed separately (Fig. 6B). K_1 was, on average, more than 2 times higher for ^{11}C-DWAY, whereas the k_2 was about half that of ^{11}C-WAY. The outliers on the K_1 graphs (Fig. 6A) correspond to regions of a single subject (subject 1). The nonspecific volume of distribution ($V_{ns} = K_1/k_2$), calculated for each ROI and PET measurement, was accordingly much higher for ^{11}C-DWAY than for ^{11}C-WAY (Table 1), whereas k_3 and k_4 were similar for the 2 radioligands (Table 1; Fig. 6A). The corresponding figures for the cerebellum (Fig. 6B) were similar to the other regions in terms of K_1 and k_2. The ratio of k_5 to k_6 supported a lower nonspecific binding for ^{11}C-DWAY than for ^{11}C-WAY but was limited by the small number of data points.

The time–activity curve for the cerebellum was better described by the 3-CM than 2-CM for both radioligands (Table 2). At the statistical evaluation, root mean square errors, Akaike information criteria scores, and Schwartz criteria scores were lower for the 3-CM than the 2-CM (Table 2). F statistics (P [T $\leq$ t], 2-tailed) rejected the null
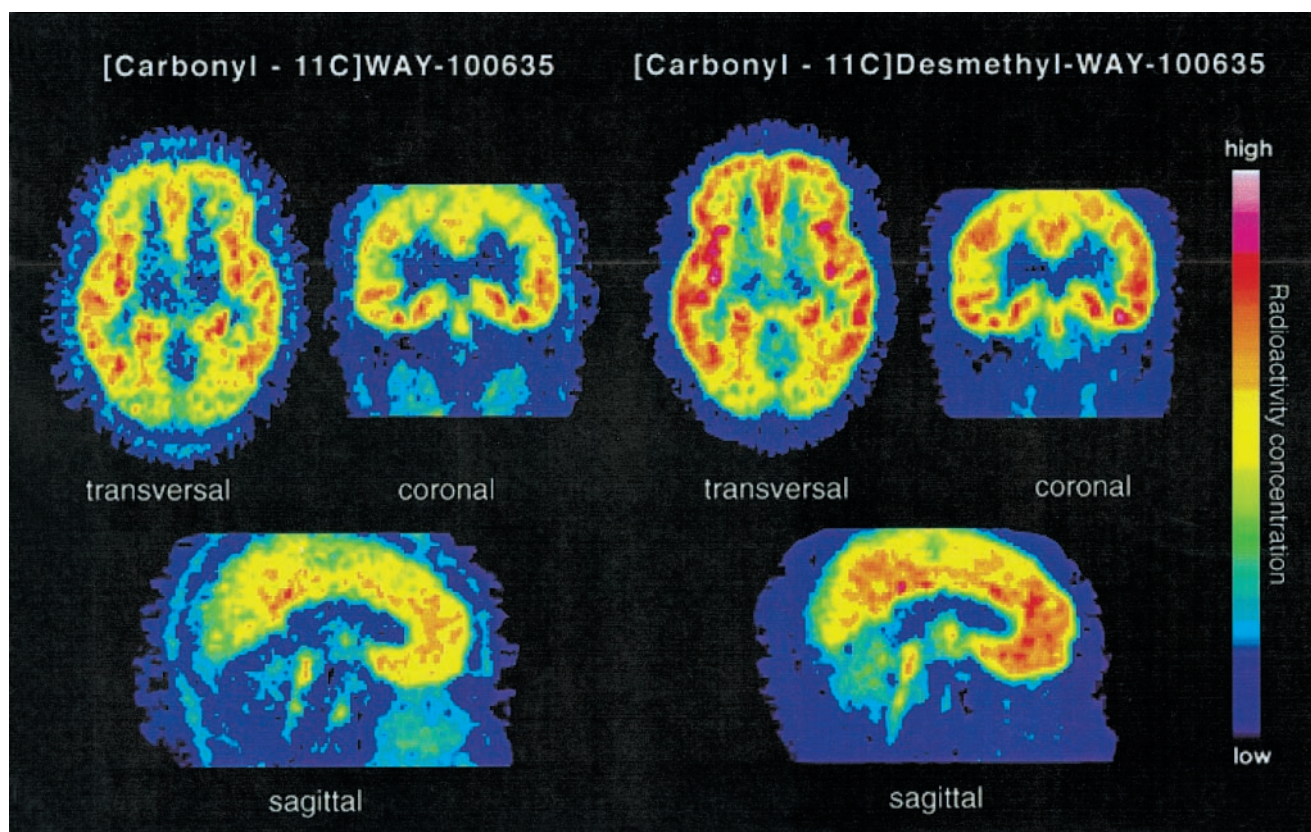

FIGURE 4. PET images in 3 projections of healthy male volunteer (subject 4), obtained by summation of frames acquired from 9 to 69 min after intravenous injection of ^{11}C-WAY and ^{11}C-DWAY, normalized to injected dose. Subject's right is on left in transaxial and coronal projections. Anterior is on right in sagittal projection.
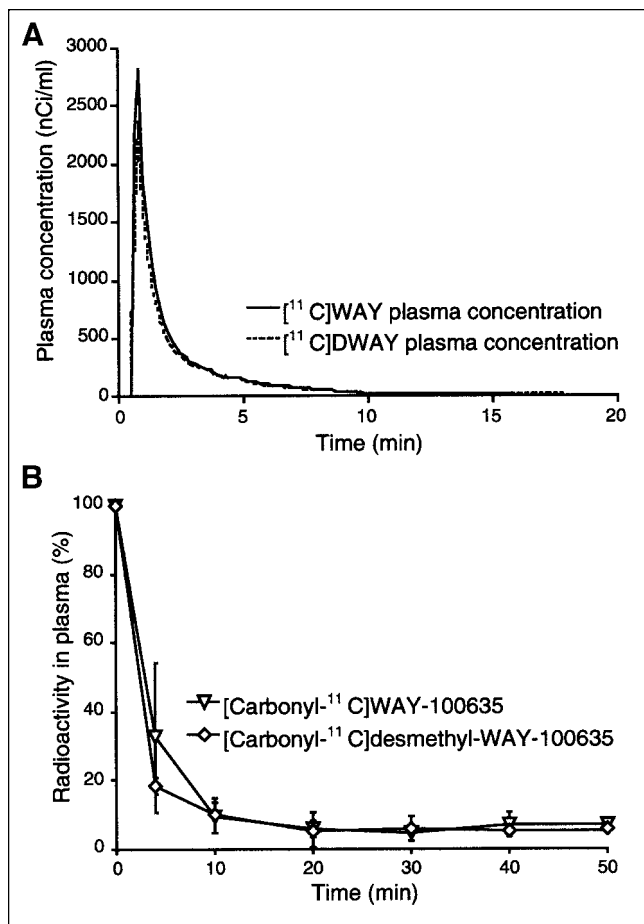
FIGURE 5. (A) Mean ($n = 5$) ^{11}C-WAY and ^{11}C-DWAY plasma concentration, normalized to injected dose and corrected for metabolites, during 69-min interval after radioligand injection. (B) Time–activity curves for fraction of radioactivity in plasma represent unchanged ^{11}C-WAY and ^{11}C-DWAY.

hypothesis for all subjects but one (^{11}C-DWAY, subject 4), thus excluding the possibility that radioligand uptake could be more adequately described by the 2-CM. The ratio of k_5 to k_6 for the cerebellum (nonspecific BP [BP_{ns}]) was lower for ^{11}C-DWAY than for ^{11}C-WAY (Table 2).

The specific binding for all regions reached a peak within the 69-min time span of the PET measurements (Figs. 3C and 3D), thus satisfying a condition for peak equilibrium. The peak was reached earlier for ^{11}C-WAY than for ^{11}C-DWAY (Fig. 3).

Regional BPs obtained by the kinetic 3-CM analysis (BP_{3-CM}), the simplified reference tissue model (BP_{SRTM}), and the peak equilibrium method (BP_{EQ}) are presented in Table 3 and Figure 7.

For both radioligands, the 3-CM gave higher values than did the simplified reference tissue model. The BP was also higher for ^{11}C-WAY when calculated by the 3-CM than when calculated by the peak equilibrium method, whereas the opposite was found for ^{11}C-DWAY (Fig. 7).

DISCUSSION

In each of the 5 subjects examined, radioactivity uptake in brain was rapid and high after intravenous administration of ^{11}C-WAY and ^{11}C-DWAY (Figs. 3 and 4). The maximal radioactivity uptake in the brain at 8 and 4 min after injection was considerably higher using ^{11}C-DWAY (mean $\pm$ SD [$n = 5$], 11.2% $\pm$ 1.9%) than using ^{11}C-WAY (4.6% $\pm$ 1.9%). The higher radioligand brain delivery and higher uptake in the cerebellum at late time points (Fig. 3) imply that ^{11}C-DWAY should provide better imaging statistics than ^{11}C-WAY at a given radioactivity dose injected.

Comparison of rate constants obtained by the 3-compartment analysis revealed a consistently higher K_1 value for ^{11}C-DWAY than for ^{11}C-WAY (Table 2; Fig. 6) and a higher nonspecific volume of distribution (V_{ns}), as shown in Table 1. The explanation for these findings may include a difference in lipophilicity, protein binding, or other factors for the 2 radioligands. Higher lipophilicity may be associated with a higher extraction of the tracer, consistent with increased delivery (K_1) and increased nonspecific binding, manifested as a reduction in k_2 in the 3-CM (k_2 in the 3-CM is a composite rate constant that includes the volume of distribution of the nonspecific compartment). However, the lipophilicity for ^{11}C-DWAY and ^{11}C-WAY has been determined (36) and does not support a higher log probability value for ^{11}C-DWAY (2.77) than for ^{11}C-WAY (26). Another explanation is a difference in the degree of plasma proteins, which have been shown to influence radioligand delivery (K_1) (22). This hypothesis could not, however, be confirmed without the associated assays, which were not determined in this study.

For both radioligands, the highest radioactivity concentration was observed in the medial temporal cortex (including the hippocampal formation), neocortex, and raphe, whereas radioactivity uptake was low but conspicuous in the cerebellar cortex (Figs. 3 and 4). The rank order for regional radioactivity is consistent with the central 5-HT$_{1A}$ receptor distribution previously reported for in vitro studies (7,37), for messenger RNA animal studies (31), and for postmortem human autoradiography studies using ^{3}H-WAY and ^{11}C-DWAY (9,18).

A possible difference in affinity for 5-HT$_{1A}$ receptors should be expected to give different levels of specific radioligand binding in the brain. ^{11}C-WAY and ^{11}C-DWAY have both been developed as putative selective antagonist radioligands with a high affinity to 5-HT$_{1A}$ receptor in the brain. They have not, however, been characterized using the same methods. WAY-100635 has been characterized using recombinant human 5-HT$_{1A}$ receptors, expressed in a Chinese hamster ovary cell line (38). Scatchard analyses have revealed a homogeneous population of ^{3}H-WAY recognition sites (K_d = 0.32 nmol/L; B_{max} = 162 fmol/mg of protein). The affinity of ^{11}C-DWAY for the 5-HT$_{1A}$ receptor subtype has been reported as an IC$_{50}$ value of 1.4 nmol/L in

TABLE 1
Parameters Obtained by Kinetic Analysis of ^{11}C-WAY and ^{11}C-DWAY Binding

Region	^{11}C-WAY 3-CM				^{11}C-DWAY 3-CM			
	K_1	k_2	k_3	k_4	K_1	k_2	k_3	k_4
Frontal cx	0.14 ± 0.05	0.25 ± 0.09	0.17 ± 0.03	0.02 ± 0.00	0.35 ± 0.06	0.15 ± 0.07	0.12 ± 0.05	0.02 ± 0.01
Ant cingulate	0.14 ± 0.05	0.25 ± 0.10	0.19 ± 0.04	0.02 ± 0.01	0.36 ± 0.04	0.17 ± 0.09	0.14 ± 0.06	0.02 ± 0.01
Temporal cx	0.14 ± 0.06	0.24 ± 0.10	0.17 ± 0.02	0.02 ± 0.00	0.35 ± 0.06	0.14 ± 0.06	0.12 ± 0.04	0.02 ± 0.01
Insular cx	0.15 ± 0.05	0.26 ± 0.11	0.20 ± 0.03	0.02 ± 0.00	0.37 ± 0.08	0.16 ± 0.08	0.15 ± 0.06	0.02 ± 0.01
Hippocampus	0.11 ± 0.04	0.15 ± 0.08	0.21 ± 0.03	0.03 ± 0.02	0.26 ± 0.05	0.09 ± 0.05	0.14 ± 0.05	0.02 ± 0.01
Raphe	0.12 ± 0.05	0.54 ± 0.55	0.24 ± 0.23	0.01 ± 0.01	0.28 ± 0.05	0.13 ± 0.10	0.09 ± 0.05	0.02 ± 0.01
Cerebellar cx	0.16 ± 0.06	0.33 ± 0.09	0.03 ± 0.01*	0.04 ± 0.01†	0.38 ± 0.08	0.17 ± 0.05	0.02 ± 0.01*	0.05 ± 0.03†

Region		CV (%)					CV (%)		
	V_{ns} (K_1/k_2)	K_1	k_2	k_3	k_4	V_{ns} (K_1/k_2)	K_1	k_2	k_3	k_4
Frontal cx	0.57 ± 0.22	39	36	18	17	2.85 ± 1.77	19	45	40	26
Ant cingulate	0.58 ± 0.20	35	39	20	26	2.88 ± 1.82	12	55	42	39
Temporal cx	0.63 ± 0.22	39	40	13	20	3.10 ± 1.85	18	43	34	30
Insular cx	0.61 ± 0.28	32	41	17	17	3.06 ± 1.92	21	48	40	31
Hippocampus	1.02 ± 0.68	38	52	49	74	3.95 ± 2.67	18	52	38	46
Raphe	0.70 ± 0.68	43	104	94	87	3.04 ± 1.66	19	76	56	41
Cerebellar cx	0.49 ± 0.21	37	27	36*	35†	2.48 ± 1.17	23	32	58*	65†

*k_5.
†k_6.
cx = cortex; ant = anterior; CV = coefficient of variance.
Values are mean ± SD ($n = 5$).

rat brain in vitro (*18*). Comparison of affinity data for ^{11}C-WAY and ^{11}C-DWAY is thus complicated by the different methods applied for the characterization of the same radioligand. A similar affinity in vivo is supported by the current observation that both radioligands provided similar BPs in regions known to contain 5-HT$_{1A}$ receptors. A difference in affinity of the 2 radioligands cannot, however, be excluded, because peak equilibrium was reached sooner for ^{11}C-WAY than for ^{11}C-DWAY (Figs. 3A and 3B).

The 3 quantitative methods gave similar BPs for ^{11}C-DWAY and ^{11}C-WAY (Table 3; Fig. 7) and, except in the raphe, with the same rank order for all subjects. Estimates of the regional BPs were higher when calculated by the 3-CM than by the 2 reference tissue approaches, which provided similar values (Table 3; Fig. 7) (*39,40*). The simplified reference tissue model and the peak equilibrium method are dependent on the cerebellum as a reference region, suggesting that the use of a reference region may provide lower BPs. This possibility calls for a critical analysis of uptake for both ^{11}C-WAY and ^{11}C-DWAY in the cerebellum.

For both radioligands, the 3-CM yielded a statistically better fit to the cerebellar data than did the 2-CM (Table 2), as supported by nonlinear least squares fitting analyses and statistical methods to select the most appropriate model. The higher estimates of BPs given by a kinetic 3-CM analysis (BP$_{3-CM}$) than by the simplified reference tissue model (BP$_{SRTM}$) or the peak equilibrium method (BP$_{EQ}$) may be explained by the additional compartment in the cerebel-

lum. This compartment will be viewed as part of the free radioligand concentration using any of the 2 reference tissue models, a simplification that will give lower BPs in regions with 5-HT$_{1A}$ receptors.

A basic assumption of the reference tissue model is that the reference tissue can be described by a 2-CM. However, the reference tissue could not be fitted to a 2-CM (Table 2). This observation does not, however, automatically mean that the 3-compartment analysis is better, because the compartment analysis does not include kinetically distinguishable nonspecific binding. When a 3-CM is applied, kinetically distinguishable nonspecific binding will thus contribute by unknown proportions to C$_b$ and Cf. The handling of data that include kinetically distinguishable nonspecific binding should thus be viewed as an accuracy problem in most currently applied quantitative approaches.

The fraction of plasma radioactivity corresponding to each of the 2 unchanged compounds, ^{11}C-WAY and ^{11}C-DWAY (Fig. 5A), was determined with HPLC for each subject and PET measurement, as described previously (*11,13*). Metabolism was rapid for both radioligands (Figs. 5A and 5B). For ^{11}C-WAY, the additional metabolite, which comigrated with reference DWAY, was previously estimated to be <2% of the parent radioligand. The value is low, but so is the percentage of ^{11}C-WAY remaining at 10 min (*13*). A small fraction of radiolabeled DWAY may be a reason for the higher BP$_{ns}$ with ^{11}C-WAY than with ^{11}C-DWAY. Given the common formation of the ^{11}C-cy-

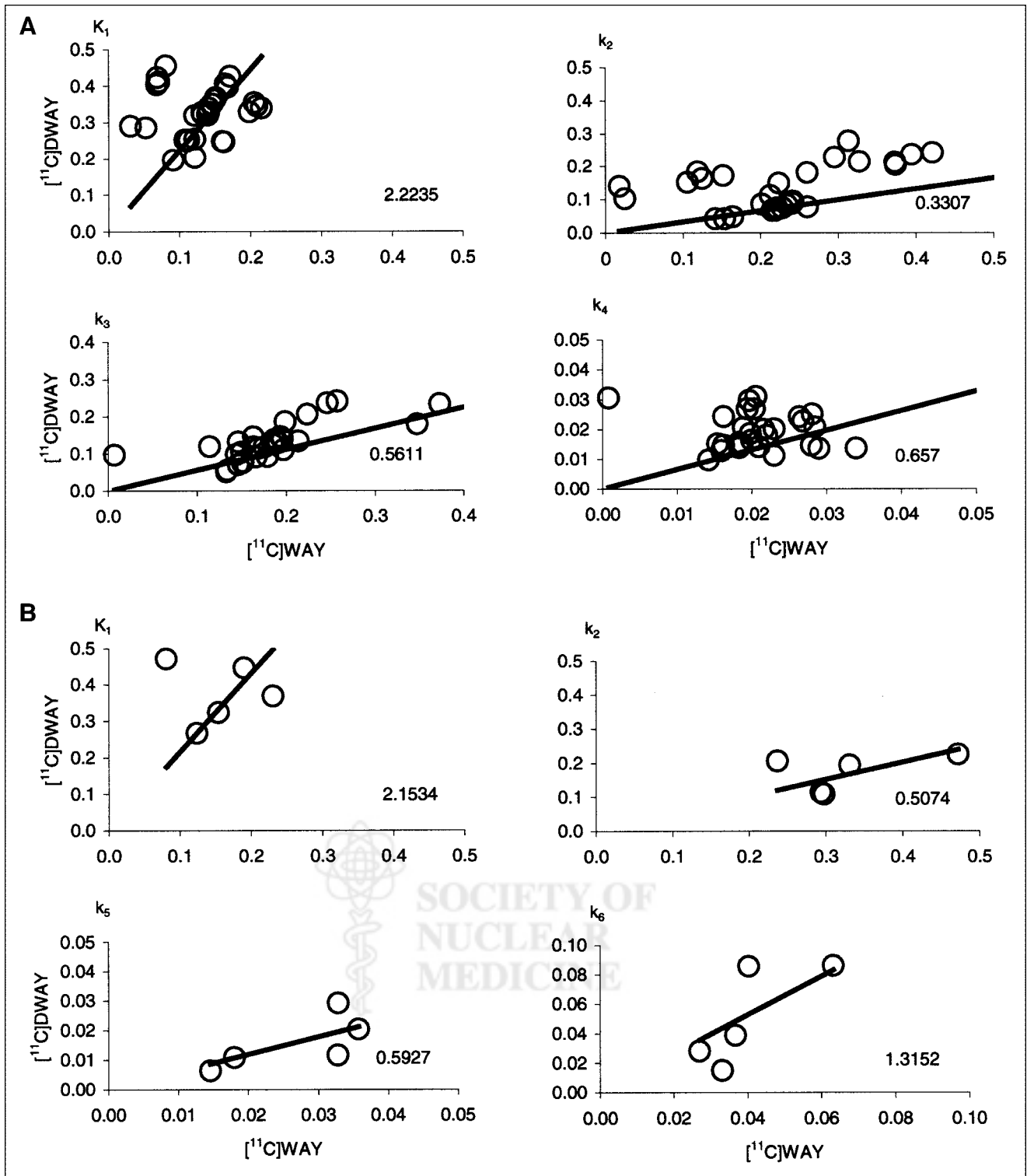**FIGURE 6.** (A) Fitted regression lines for rate constants (K_1, k_2, k_3, and k_4) for 6 central 5-HT$_{1A}$ receptor-rich regions determined by kinetic 3-CM analysis for ^{11}C-WAY (*x*-axis) and ^{11}C-DWAY (*y*-axis) at a certain radioactivity concentration. (B) Corresponding fitted regression lines for rate constants (K_1, k_2, k_5, and k_6) in cerebellum.

TABLE 2
Comparison of 2-CM and 3-CM for Description of ^{11}C-WAY and ^{11}C-DWAY Binding in Cerebellum of 5 Healthy Subjects

Subject no.	Compound	Model	K_1 (mg/mL/min)	k_2 (min^{-1})	k_5 (min^{-1})	k_6 (min^{-1})	BP$_{ns}$ (k_5/k_6)	RMS error	AIC	SC	F statistic
1	^{11}C-WAY	2-CM	0.077	0.195	—	—	—	11	125	126	$P < 0.05$
		3-CM	0.081	0.237	0.018	0.027	0.675	8	118	121	
	^{11}C-DWAY	2-CM	0.451	0.178	—	—	—	32	159	161	$P < 0.05$
		3-CM	0.471	0.206	0.011	0.028	0.385	23	152	155	
2	^{11}C-WAY	2-CM	0.172	0.214	—	—	—	23	148	150	$P < 0.00005$
		3-CM	0.190	0.298	0.033	0.033	0.988	10	124	128	
	^{11}C-DWAY	2-CM	0.419	0.085	—	—	—	11	162	163	$P < 0.01$
		3-CM	0.446	0.109	0.011	0.015	0.766	23	153	156	
3	^{11}C-WAY	2-CM	0.137	0.345	—	—	—	10	123	125	$P < 0.001$
		3-CM	0.154	0.472	0.036	0.037	0.972	6	108	111	
	^{11}C-DWAY	2-CM	0.297	0.174	—	—	—	13	130	131	$P < 0.05$
		3-CM	0.324	0.226	0.020	0.039	0.526	9	124	127	
4	^{11}C-WAY	2-CM	0.222	0.259	—	—	—	15	135	137	$P < 0.05$
		3-CM	0.231	0.294	0.015	0.040	0.362	11	130	133	
	^{11}C-DWAY	2-CM	0.363	0.107	—	—	—	20	145	146	NS
		3-CM	0.368	0.114	0.006	0.086	0.074	20	148	151	
5	^{11}C-WAY	2-CM	0.115	0.256	—	—	—	9	120	121	$P < 0.00005$
		3-CM	0.124	0.331	0.033	0.063	0.519	3	87	90	
	^{11}C-DWAY	2-CM	0.252	0.154	—	—	—	13	130	131	$P < 0.00005$
		3-CM	0.267	0.194	0.029	0.086	0.339	6	109	112	

RMS = root mean square; AIC = Akaike information criteria; SC = Schwartz criteria; NS = not significant.

For F statistics, null hypothesis was that 2-compartment model more adequately describes radioligand uptake. *P* describes level on which null hypothesis was rejected.

clohexanecarboxylic acid (*11*) using ^{11}C-WAY as well as ^{11}C-DWAY, this labeled metabolite may explain the need for a 3-CM to describe cerebellar radioactivity in kinetic analyses for both radioligands.

The main objective of this study was to evaluate prospects for using ^{11}C-DWAY as an alternative to ^{11}C-WAY. We used 3 analytic methods as tools to describe the new radioligand in this first study on humans. The set of methods was not primarily used to choose the best method for applied studies with any of the tracers. Studies on larger

samples are required for that purpose. However, taking advantage of such information from studies with the reference ligand ^{11}C-WAY, we have approached the demand by inclusion of a new figure (Fig. 7). From such a comparison of BPs derived from invasive (3-CM) and noninvasive (peak equilibrium and SRTM) reference tissue models using the cerebellum as reference region and input function, respectively, use of a noninvasive method can be recommended for studies in which interindividual differences in nonspecific binding are of little concern. Similarly, BPs

TABLE 3
Binding Potentials for ^{11}C-WAY and ^{11}C-DWAY Calculated by 3 Quantitative Approaches

Region	^{11}C-WAY BP$_{3\text{-CM}}$ VD	^{11}C-WAY BP$_{3\text{-CM}}$ V/V$_{cerebellum}$ − 1	^{11}C-WAY BP$_{SRTM}$	^{11}C-WAY BP$_{EQ}$	^{11}C-DWAY BP$_{3\text{-CM}}$ VD	^{11}C-DWAY BP$_{3\text{-CM}}$ V/V$_{cerebellum}$ − 1	^{11}C-DWAY BP$_{SRTM}$	^{11}C-DWAY BP$_{EQ}$
Frontal cx	4.74 ± 2.21	4.76 ± 1.28	3.36 ± 1.08	3.38 ± 2.57	17.65 ± 6.60	4.33 ± 0.91	4.20 ± 1.26	4.67 ± 1.67
Ant cingulate	5.16 ± 2.25	5.36 ± 1.46	3.74 ± 1.20	3.17 ± 0.96	21.38 ± 7.63	5.52 ± 1.18	5.19 ± 1.50	5.88 ± 2.20
Temporal cx	5.47 ± 2.56	5.69 ± 1.61	3.95 ± 1.33	3.46 ± 1.42	20.67 ± 7.25	5.31 ± 1.24	4.83 ± 1.43	6.29 ± 2.03
Insulate	6.91 ± 3.42	7.45 ± 2.29	4.87 ± 1.62	3.91 ± 1.29	24.98 ± 7.81	6.75 ± 1.72	6.13 ± 1.90	7.37 ± 2.59
Hippocampus	8.13 ± 3.49	8.95 ± 1.95	5.17 ± 1.41	5.63 ± 2.01	31.72 ± 8.67	9.03 ± 2.55	6.38 ± 2.05	7.73 ± 2.42
Raphe	12.98 ± 18.02	17.55 ± 28.64	6.14 ± 6.17	8.77 ± 8.07	16.84 ± 5.67	4.45 ± 2.38	4.74 ± 3.28	9.05 ± 6.60
Cerebellum	0.82 ± 0.32	NA	NA	NA	3.57 ± 2.14	NA	NA	NA

VD = volume of distribution; cx = cortex; ant = anterior; NA = not applicable.

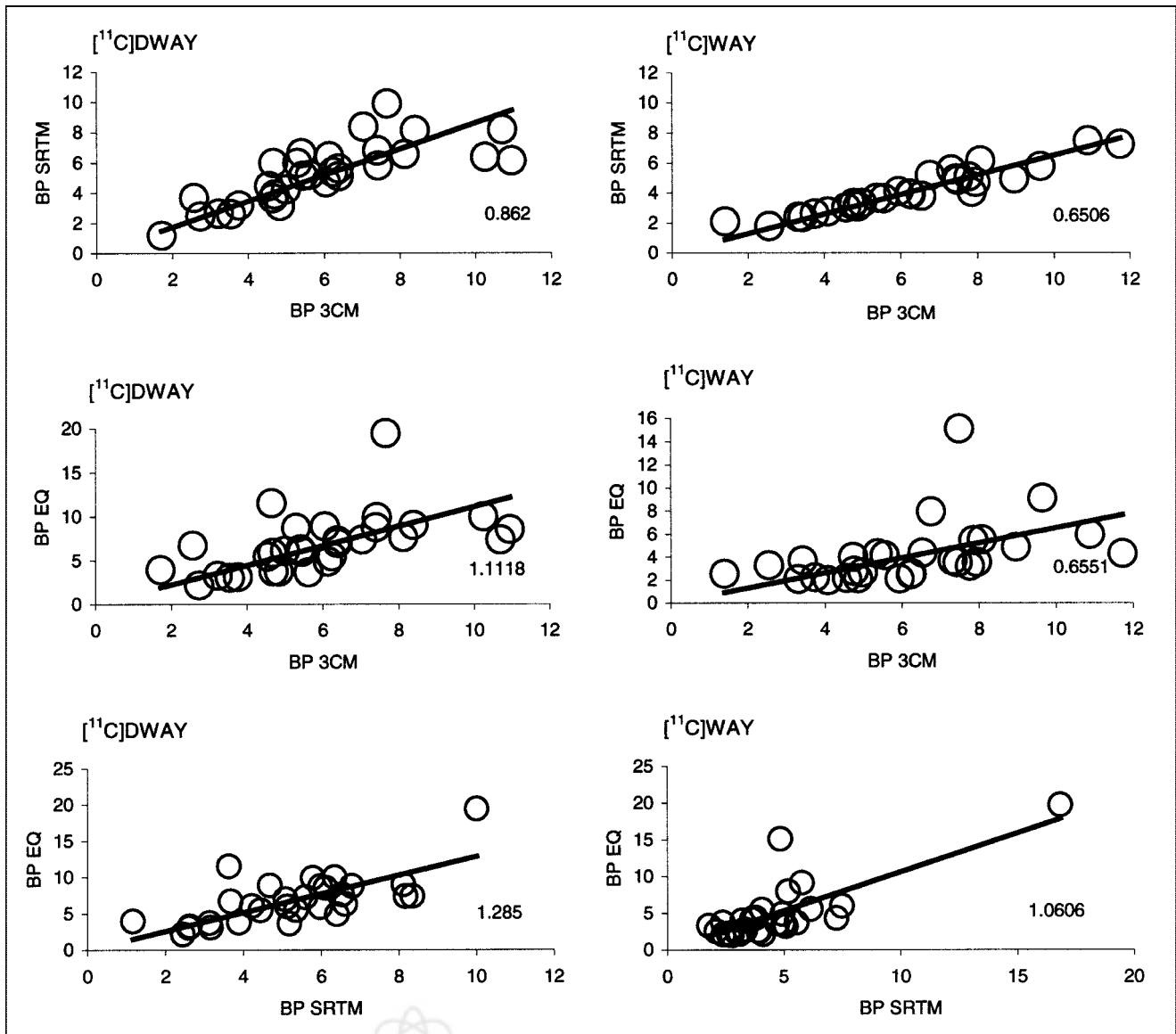Values are mean ± SD (*n* = 5). V/V$_{cerebellum}$ − 1 corresponds to binding potential (BP).

FIGURE 7. Fitted regression lines for regional BPs in 6 central regions in 5 healthy male volunteers calculated by kinetic 3-compartment analysis ($BP_{3\text{-}CM}$), simplified reference tissue model (BP_{SRTM}), and peak equilibrium method (BP_{EQ}), respectively.

derived from the distribution volume using a plasma input may be recommended if there are concerns about changes in nonspecific binding and if measures for plasma protein binding are available.

CONCLUSION

The ^{11}C-DWAY PET radioligand provides 2-fold higher brain uptake than does ^{11}C-WAY. This is a putative advantage over ^{11}C-WAY for quantification and labeling of 5-HT$_{1A}$ receptors in the human brain, implicating better imaging statistics and advantages in biomathematic modeling. Differences in lipophilicity or protein binding are suggested as plausible explanations for the difference in brain uptake between the 2 radioligands. The beneficial metabo-

lism of ^{11}C-DWAY, which limits the formation of possible active metabolites, and a smaller kinetically distinguishable nonspecific binding compartment in the cerebellum for ^{11}C-DWAY than for ^{11}C-WAY, which is indicated by a kinetic 3-CM analysis, further support the suitability of ^{11}C-DWAY as a PET radioligand for measures of 5-HT$_{1A}$ receptors in the human brain.

REFERENCES

1. Farde L. PET in neuropsychiatric drug development. In: Comar D, ed. *PET for Drug Development and Evaluation*. Vol 26. Dordrecht, The Netherlands: Kluwer Academic Publishers; 1995:51–92.

2. Artigas F, Perez V, Alvarez E. Pindolol induces a rapid improvement of depressed patients treated with serotonin reuptake inhibitors [letter]. *Arch Gen Psychiatry.* 1994;51:248–251.

3. Assie MB, Cosi C, Koek W. 5-HT$_{1A}$ receptor agonist properties of the antipsychotic, nemonapride: comparison with bromerguride and clozapine. *Eur J Pharmacol.* 1997;334:141–147.

4. Millan MJ, Hjorth S, Samanin R, et al. S 15535, a novel benzodioxopiperazine ligand of serotonin 5-HT$_{1A}$ receptors. II. Modulation of hippocampal serotonin release in relation to potential anxiolytic properties. *J Pharmacol Exp Ther.* 1997;282:148–161.

5. Newman-Tancredi A, Gavaudan S, Conte C, et al. Agonist and antagonist actions of antipsychotic agents at 5-HT$_{1A}$ receptors: a [^{35}S]GTPgammaS binding study. *Eur J Pharmacol.* 1998;355:245–256.

6. Hjorth S, Sharp T. Effect of the 5-HT$_{1A}$ receptor agonist 8-OH-DPAT on the release of 5-HT in dorsal and median raphe-innervated rat brain regions as measured by in vivo microdialysis. *Life Sci.* 1991;48:1779–1786.

7. Pazos A, Probst A, Palacios JM. Serotonin receptors in the human brain. III. Autoradiographic mapping of serotonin-1 receptors. *Neuroscience.* 1987;21:97–122.

8. Khawaja X. Quantitative autoradiographic characterisation of the binding of [^{3}H]WAY-100635, a selective 5-HT$_{1A}$ receptor antagonist. *Brain Res.* 1995;673:217–225.

9. Hall H, Lundkvist C, Halldin C, et al. Autoradiographic localization of 5-HT$_{1A}$ receptors in the post-mortem human brain using [^{3}H]WAY-100635 and [^{11}C]WAY-100635. *Brain Res.* 1997;745:96–108.

10. Pike VW, McCarron JA, Lammertsma AA, et al. Exquisite delineation of 5-HT$_{1A}$ receptors in human brain with PET and [*carbonyl*-^{11}C]WAY-100635. *Eur J Pharmacol.* 1996;301:R5–R7.

11. Osman S, Lundkvist C, Pike VW, et al. Characterisation of the appearance of radioactive metabolites in monkey and human plasma from the 5-HT$_{1A}$ receptor radioligand, [*carbonyl*-^{11}C]WAY-100635: explanation of high signal contrast in PET and an aid to biomathematical modelling. *Nucl Med Biol.* 1998;25:215–223.

12. Farde L, Ginovart N, Ito H, et al. PET-characterization of [*carbonyl*-^{11}C]WAY-100635 binding to 5-HT$_{1A}$ receptors in the primate brain. *Psychopharmacology.* 1997;133:196–202.

13. Farde L, Ito H, Swahn CG, Pike VW, Halldin C. Quantitative analyses of carbonyl-carbon-11-WAY-100635 binding to central 5-hydroxytryptamine-1A receptors in man. *J Nucl Med.* 1998;39:1965–1971.

14. Gunn RN, Sargent PA, Bench CJ, et al. Tracer kinetic modeling of the 5-HT$_{1A}$ receptor ligand [*carbonyl*-^{11}C]WAY-100635 for PET. *Neuroimage.* 1998;8:426–440.

15. Parsey RV, Slifstein M, Hwang DR, et al. Validation and reproducibility of measurement of 5-HT$_{1A}$ receptor parameters with [*carbonyl*-^{11}C]WAY-100635 in humans: comparison of arterial and reference tissue input functions. *J Cereb Blood Flow Metab.* 2000;20:1111–1133.

16. Osman S, Lundkvist C, Pike VW, et al. Characterization of the radioactive metabolites of the 5-HT$_{1A}$ receptor radioligand, [O-methyl-^{11}C]WAY-100635, in monkey and human plasma by HPLC: comparison of the behaviour of an identified radioactive metabolite with parent radioligand in monkey using PET. *Nucl Med Biol.* 1996;23:627–634.

17. Carson R, Schmall B, Endres C, et al. Kinetic modelling of the 5-HT$_{1A}$ antagonist [carbonyl-^{11}C]-WAY-100635. *J Cereb Blood Flow Metab.* 1997;17(suppl):S327.

18. Pike VW, Halldin C, McCarron JA, et al. [*carbonyl*-^{11}C]Desmethyl-WAY-100635 (DWAY) is a potent and selective radioligand for central 5-HT$_{1A}$ receptors in vitro and in vivo. *Eur J Nucl Med.* 1998;25:338–346.

19. Farde L, Halldin C, Andrée B, Swahn C-G, Sandell J, Pike VW. DWAY is a selective radioligand for human brain 5-HT$_{1A}$ receptors in vivo and gives a more intense signal than WAY. *J Labelled Compds Radiopharm.* 1999;42(suppl 1):S63–S65.

20. Bergström M, Boëthius J, Eriksson L, Greitz T, Ribbe T, Widén L. Head fixation device for reproducible position alignment in transmission CT and positron emission tomography. *J Comput Assist Tomogr.* 1981;5:136–141.

21. Eriksson L, Holte S, Bohm C, Kesselberg M, Hovander B. Automated blood sampling systems for positron emission tomography. *IEEE Trans Nucl Sci.* 1988;35:703–707.

22. Farde L, Eriksson L, Blomquist G, Halldin C. Kinetic analysis of central [^{11}C]raclopride binding to D$_2$-dopamine receptors studied by PET: a comparison to the equilibrium analysis. *J Cereb Blood Flow Metab.* 1989;9:696–708.

23. Wienhard K, Dahlbom M, Eriksson L, et al. The ECAT EXACT HR: performance of a new high resolution positron scanner. *J Comput Assist Tomogr.* 1994;18:110–118.

24. Wong D, Gjedde A, Wagner H Jr. Quantification of neuroreceptors in the living human brain. I. Irreversible binding of ligands. *J Cereb Blood Flow Metab.* 1986;6:137–146.

25. Mintun M, Raichle M, Kilbourn M, Wooten G, Welch M. A quantitative model for the *in vivo* assessment of drug binding sites with positron emission tomography. *Ann Neurol.* 1984;15:217–227.

26. Huang S, Barrio J, Phelps M. Neuroreceptor assay with positron emission tomography: equilibrium versus dynamic approaches. *J Cereb Blood Flow Metab.* 1986;6:515–521.

27. Marquardt D. An algorithm for least-squares estimation of nonlinear parameters. *J Soc Ind Appl Math.* 1963:431–441.

28. Lammertsma AA, Bench CJ, Hume SP, et al. Comparison of methods for analysis of clinical [^{11}C]raclopride studies. *J Cereb Blood Flow Metab.* 1996;16:42–52.

29. Burnet PW, Eastwood SL, Harrison PJ. [^{3}H]WAY-100635 for 5-HT$_{1A}$ receptor autoradiography in human brain: a comparison with [^{3}H]8-OH-DPAT and demonstration of increased binding in the frontal cortex in schizophrenia. *Neurochem Int.* 1997;30:565–574.

30. Lammertsma AA, Hume SP. Simplified reference tissue model for PET receptor studies. *Neuroimage.* 1996;4:153–158.

31. Burnet PW, Eastwood SL, Lacey K, Harrison PJ. The distribution of 5-HT$_{1A}$ and 5-HT$_{2A}$ receptor mRNA in human brain. *Brain Res.* 1995;676:157–168.

32. Hawkins R, Phelps M, Huang S-C. Effects of temporal sampling, glucose metabolic rates, and disruptions of the blood-brain barrier on the FDG model with and without a vascular compartment: studies in human brain tumors with PET. *J Cereb Blood Flow Metab.* 1986;6:170–183.

33. Akaike H. A new look at the statistical model identification. *IEEE Trans Automat Contr.* 1974;19:716–723.

34. Schwartz G. Estimating the dimension of a model. *Ann Stat.* 1978;6:461–564.

35. Phelps M, Huang S, Hoffman E, Selin C, Sokoloff L, Kuhl D. Tomographic measurement of local cerebral glucose metabolic rate in humans with (F-18)2-fluoro-2-deoxy-D-glucose: validation of method. *Ann Neurol.* 1979;6:371–388.

36. Pike VW, Halldin C, Wikstrom H. Radioligands for the study of brain 5-HT$_{1A}$ receptors in vivo. In: *Progress in Medical Chemistry*. Amsterdam, The Netherlands: Elsevier Science BV; 2000:187–247.

37. Hoyer D, Pazos A, Probst A, Palacios JM. Serotonin receptors in the human brain. I. Characterization and autoradiographic localization of 5-HT$_{1A}$ recognition sites: apparent absence of 5-HT$_{1B}$ recognition sites. *Brain Res.* 1986;376:85–96.

38. Khawaja X, Ennis C, Minchin MC. Pharmacological characterization of recombinant human 5-hydroxytryptamine1A receptors using a novel antagonist radioligand, [3H]WAY-100635. *Life Sci.* 1997;60:653–665.

39. Gunn RN, Lammertsma AA, Grasby PM. Quantitative analysis of [*carbonyl*-^{11}C]WAY-100635 PET studies. *Nucl Med Biol.* 2000;27:477–482.

40. Slifstein M, Parsey RV, Laruelle M. Derivation of [^{11}C]WAY-100635 binding parameters with reference tissue models: effect of violations of model assumptions. *Nucl Med Biol.* 2000;27:487–492.